

# A Hybrid High speed Electrical Micromachine for Micro Scale Power Generation

S. Stevens, *Student Member, IEEE*, J. Driesen, *Member, IEEE* and R. Belmans, *Fellow, IEEE*  
 K.U.Leuven - ESAT, div. ELECTA  
 Kasteelpark Arenberg 10, 3001 Heverlee, Belgium

**Abstract**—This paper presents a methodology for the optimization of a new type of high speed electrical micromachine for micro scale power generation. The micromachine is integrated into the compressor of a microturbine which operates at 500,000  $r/min$  [1]–[3]. Because of the high energy density of fuel, the turbine-generator combination exceeds the limitations of batteries and smoothes the way for high power or long endurance applications. The micromachine is optimized for a mechanical output power of 100 W within the dimensions of the turbine. Special attention is paid to the problems caused by high speed operation and their influence on the design of the machine.

**Index Terms**—Microelectromechanical devices, micromotor, Permanent magnet generator, Transient analysis

## I. INTRODUCTION

Most portable and unmanned devices use batteries for their power supply. Currently Li-ion batteries have energy densities up to 0.5 MJ/kg, but not only do they offer limited autonomy, also charging times pose a problem. Fuel based power generation on the other hand offers an energetic density of about 45 MJ/kg, and the fuel reservoir can easily be refilled. Even with energy efficiencies as low as 2 %, this combination provides a solution for many applications which require higher energy density than batteries can offer e.g. for portable communication systems, communication systems in UAV's (Unmanned Aerial Vehicles), laptops or portable electrical power generator.

In order to exceed the energy density of batteries, the turbine and generator must be miniaturized and made as efficient as possible. If the power unit has to maintain the same output power when scaled down, the speed has to be increased in order to reduce the forces acting in both the turbine and generator. To generate 100 W of mechanical output power with conventional speeds requires an extreme high torque to be produced by a machine in the order of a cm in diameter. Assume that the micromachine has a rotating speed of 5,000  $r/min$ , a torque of 0.2 Nm is required to obtain 100 W of mechanical output power. If a 2-pole radial flux machine would have 20 slots and an outer radius of 1 cm, the total current through a slot must be 200 A with the air gap flux density  $B = 1$  T, the length of the machine 1 cm and ten slots active. Clearly this is not realistic, therefore the speed must

be increased. The target of this new machine is an operation speed of 500,000  $r/min$  and because this micromachine is not only a generator but it is also used to start up the turbine, the mechanical output power of 100 W is provided [4]. The electrical output power must be as large as possible.

## II. MICROMACHINE

High speeds result in high mechanical stresses, therefore a symmetric solid rotor structure is chosen which is mounted on the compressor disc, see Fig. 1. This configuration has the advantage to be very robust and the placement of the rotor directly onto the compressor avoids the use of an extra bearing which leads to higher losses. This extra bearing would have been inevitable if the micromachine was a stand alone machine with a mechanical coupling with the turbine. Due to the integration of compressor and rotor, the outer dimension of the rotor is bounded to the dimensions of the compressor in order to limit the friction loss between rotor and stator, see Fig. 1.

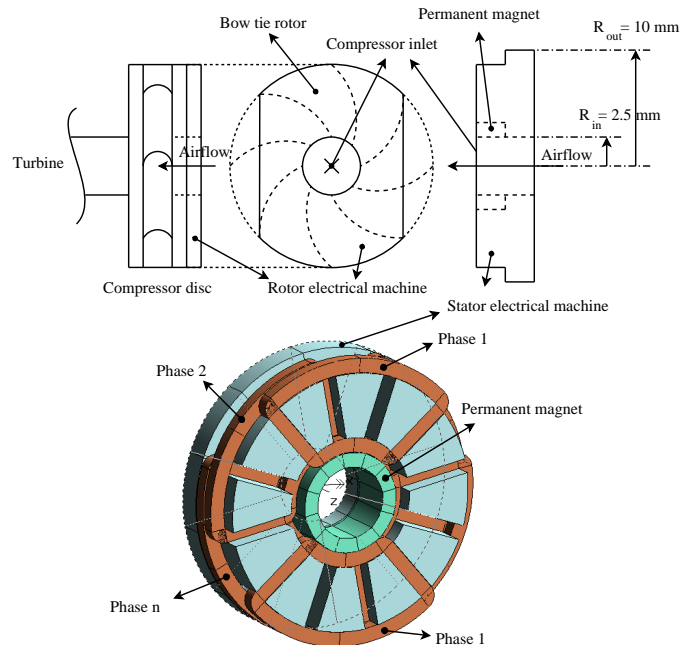


Fig. 1. Overview of the micromotor

To create a magnetic flux through the machine, there are two possibilities: coils actuated by an external energy source

This research is sponsored by the IWT, the Institute for the Promotion of Innovation by Science and Technology in Flanders, Belgium, project SBO 030288 "PowerMEMS".

or a permanent magnet. The use of coils is interesting in high temperature environments. Operating temperature is the most important drawback for permanent magnets (limited in practice to operation temperatures of 400 K). The temperature problem is reduced by placing the magnet on the lowest temperature side of the turbine (the compressor side) and by extra cooling through passing the inlet air over the permanent magnet, see Fig. 1. The permanent magnet is ring shaped and axially magnetized. All the active parts, resp. permanent magnet and coils, are placed on the stator (non-moving part), to avoid damage resulting from high stresses and friction. The magnet is in one piece, the segmentation visible in Fig. 1 is due to parametrization of the FE model.

In Fig. 2 an overview of the magnetic flux path is given. The magnet creates a flux that crosses the air gap and enters the rotor. From here it goes towards the outer diameter where it again crosses the air gap towards the stator teeth. The flux paths close via the stator back iron to the permanent magnet.

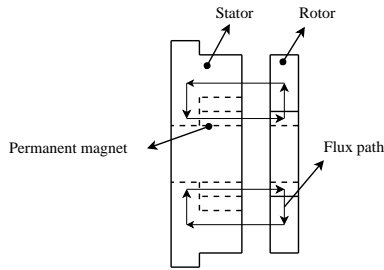


Fig. 2. Magnetic flux path

The name *hybrid* is chosen because this micromachine combines the force principles of a permanent magnet machine and of a reluctance machine. In the next sections the design methodology is explained, special attention is paid for the influences of the high speed in section IV. To finish the results of the non-linear static optimization process and the transient solution are reported.

### III. DESIGN OUTLINE

In order to avoid a time consuming optimization with finite elements (FE), an optimization process based on a FE-model combined with a fast Discrete Circuit Modelling (DCM) model is used (Fig. 3). First, the reluctances of the DCM-model are evaluated with the FE-model. Optimization is then performed on basis of the DCM-model and the final geometry is subjected to a FE analysis. If the computed performances of the machine do not match the DCM values, the optimization process is restarted with updated values of the reluctances.

#### A. System of equations

The system of equations is composed of the following set equations:

- Magnetic circuit equations
- Electrical circuit equations
- Coupling magnetic and electrical circuit

- Mechanical equations

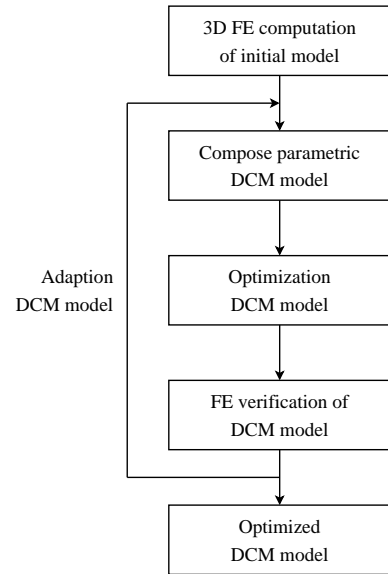


Fig. 3. Overview of the design process

The magnetic circuit equations are based upon Fig. 4 which is a simplified representation of the machine derived from the FE draft. A magnetic scalar potential is defined in each node. By using Kirchoff's current law, it is possible to write  $N - 1$  linearly independent relations for the  $N$  unknowns, with  $N$  the number of nodes. The last relation to complete the set of magnetic equations is given by the arbitrary constraint  $u_{bpm} = 0$ . Saturation is accounted for by using a linearization of the permeability of the material (iron). The reluctances which can saturate have a diagonal, see Fig. 4.

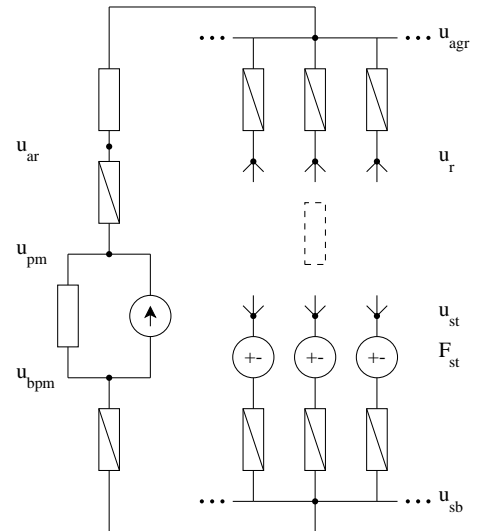


Fig. 4. The magnetic scheme

The second set of equations is based upon the electrical circuit equations. It is assumed that the electrical circuits are connected into star, this is also true for the load. The number of linear independent equations is equal to  $N_{ph}$ . The

equations consist of  $N_{ph} - 1$  Kirchoff voltage equations and 1 Kirchoff current equation. The load that is present in these equations can be resistive, capacitive or inductive. This has only its implications on the arrangement within the matrices of (3) when solving the problem.

The third set of equations gives the coupling between the magnetomotive force (mmf) of the coils and the current through it.

The last set consists of two mechanical equations:

$$\frac{d\omega}{dt} = \frac{T_{appl} + \sum_i \sum_j \mathcal{P}_{ij}(u_{st,i} - u_{r,j})^2 - k\theta - c\omega}{J_{mech}} \quad (1)$$

$$\frac{d\theta}{dt} = \omega \quad (2)$$

with

$T_{appl}$	the applied torque
$J_{mech}$	the inertia of the rotor
$k$	the spring constant (zero in this case)
$c$	the damping factor
$\theta$	the angular position of the rotor
$\omega$	the circumferential speed

The summation term represents the reluctance force. The total number of unknowns is:

$$\mathbf{X} = \begin{bmatrix} u_{magn}(N_{st} + 4 + N_r \times 1) \\ F_{st}(N_{st} \times 1) \\ i_{ph}(N_{ph} \times 1) \\ \theta(1 \times 1) \\ \omega(1 \times 1) \\ u_{pot}(N_{ph} \times 1) \\ \int idt(N_{ph} \times 1) \end{bmatrix}$$

By differentiating the magnetic circuit equations, the time dependence of the magnetic circuit is obtained. By using a three step, fifth order Runge Kutta implicit time integration scheme, the total system equations can be solved [5] [6]. The system equations look like:

$$M\dot{\mathbf{X}} + K\mathbf{X} + \mathbf{B} = 0 \quad (3)$$

### B. Magnetic circuit

As mentioned above the design is started with a draft of the final model. The dimensions are not correct but the model will help to predict the reluctances. For the FE analysis the whole machine is modelled while for the DCM analysis only the active part is used (part that is overlapped by the rotor). The result of the 3D non-linear FE computation is shown in Fig. 5. The proposed reluctance scheme is shown in Fig. 6. To calculate the reluctances, the blocks in Fig. 6 have to be revolved around the center axis to obtain the active part of the machine. The revolving angle is  $\theta$ , corresponding to the

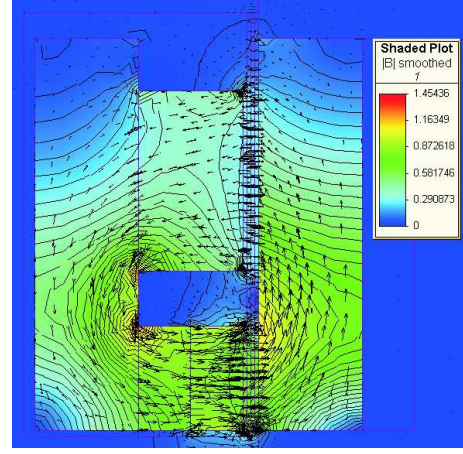


Fig. 5. 3D calculation to derive the magnetic scheme

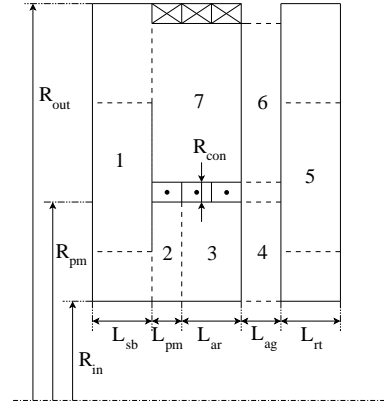


Fig. 6. The magnetic scheme

revolving angle of the rotor. Following reluctances are used:

$$\mathfrak{R}_1 = \frac{1}{\mu\theta L_{sb}} \ln\left(\frac{R_{out} + R_{pm}}{R_{pm} + R_{in}}\right) \quad (4)$$

$$\mathfrak{R}_2 = \frac{L_{pm}}{\mu_{pm} \frac{\pi}{2} (R_{pm}^2 - R_{in}^2)} \quad (5)$$

$$\mathfrak{R}_3 = \frac{L_{ar}}{\mu \frac{\pi}{2} (R_{pm}^2 - R_{in}^2)} \quad (6)$$

$$\mathfrak{R}_4 = \frac{L_{ag}}{\mu_0 \frac{\pi}{2} (R_{pm}^2 - R_{in}^2)} \quad (7)$$

$$\mathfrak{R}_5 = \frac{1}{\mu\theta L_{rt}} \ln\left(\frac{R_{out} + R_{pm}}{R_{pm} + R_{in}}\right) \quad (8)$$

$$\mathfrak{R}_6 = \frac{L_{ag}}{\mu_0 \frac{\theta}{2} [(R_{out} - R_{con})^2 - (R_{pm} + R_{con})^2]} \quad (9)$$

$$A_{con} = R_{con} [R_{out} - R_{pm} - 2R_{con}] \quad (10)$$

$$\mathfrak{R}_7 = \frac{L_{pm} + L_{ar}}{\mu \left[ \frac{\theta}{2} [(R_{out} - R_{con})^2 - (R_{pm} + R_{con})^2] - N_{slot} A_{con} \right]} \quad (11)$$

Herein is:

$R_{out}$	the outer radius of the machine
$R_{in}$	the inner radius of the machine
$R_{pm}$	the outer radius of the permanent magnet
$L_{sb}$	the width of the stator back

$L_{ar}$	additional length of PM with permeable material
$R_{con}$	width of the conductor
$L_{ag}$	the air gap length
$L_{rt}$	width of the rotor
$A_{con}$	area on stator surface occupied by a single conductor
$N_{slot}$	the number of slots overlapped by the rotor and that carry current of the same phase

#### IV. DESIGN CONSIDERATIONS

Some parameters can be optimized on the basis of a few considerations regarding machine control and eddy current losses:

- The mechanical time constant of the machine is (speed control):

$$\tau_{mech} \sim \frac{J_{mech}}{c} \quad (12)$$

In order to decrease  $J_{mech}$  and hence the time constant,  $L_{rt}$  must be kept as low as possible. Increasing  $J_{mech}$  can also be advantageous in canceling the fluctuations in the driving system or the ripple in the electrical output power.

- The electrical time constant of the machine is:

$$\tau_{elec} = \frac{L}{R} \quad (13)$$

with

$L$	the inductance
$R$	the electrical resistivity

The inductance  $L$  can be written as  $\frac{N_s^2}{\mathfrak{R}}$ . Herein is  $N_s$  the number of turns in series and  $\mathfrak{R}$  the reluctance of the system. To minimize  $\tau_{elec}$ ,  $N_s$  must be small and  $\mathfrak{R}$  must be as large as possible, which corresponds to minimizing the reluctance of the rotor (minimizing  $L_{rt}$ ) since there flows a homopolar flux through it which causes no eddy current losses. Taking  $N_s = 1$  means connecting all turns parallel with each other. This does not influence the copper losses as can be seen in following equations:

$$P_{cop,p} = 2\rho_{eff,c}(T, f)l_c N_p A_c J^2 \quad (14)$$

$$P_{cop,s} = 2N_s \rho_{eff,c}(T, f)l_c A_c J^2 \quad (15)$$

with

$\rho_{eff,c}(T, f)$	the effective specific resistivity of the conductor which depends on temperature and frequency
----------------------	--

$A_c$	the conductor area
$l_c$	the conductor length
$J$	the current density
$N_s$	the number of turns that are in series
$N_p$	the number of turns that are in parallel

In formulae (14) and (15)  $P_{cop,p}$  represents the copper loss for the parallel connection and  $P_{cop,s}$  represents the copper loss for the series connection of all turns. If a

number of turns is required, it is better to put all turns in parallel to minimize the time constant. The factor 2 in (14) and (15) comes from the fact that 2 pole pairs are used (see later).

- The losses due to eddy current are equal to:

$$P_{ec,stat} = \theta \left[ \left( \frac{R_{out} + R_{pm}}{2} \right)^2 - \left( \frac{R_{pm} + R_{in}}{2} \right)^2 \right] \cdot \dots \frac{\omega^2 \hat{B}_{stat}^2 L_{sb} V ol_{stat}}{\rho_{eff,stat}(T, f)} \quad (16)$$

$$P_{ec,teeth} = \theta \left[ (R_{out} - R_{con})^2 - (R_{pm} + R_{con})^2 \dots - N_{slot} A_{con} \right] \cdot \dots \frac{\omega^2 \hat{B}_{teeth}^2 L_{rt} V ol_{teeth}}{\rho_{eff,stat}(T, f)} \quad (17)$$

These formulae show that the electrical frequency of the machine and the magnetic flux densities in the stator teeth and back should be as small as possible to minimize the eddy current losses. This also has a positive effect on the copper losses. If the frequency is reduced,  $\rho_{eff,stat}(T, f)$  and  $\rho_{eff,c}(T, f)$  are reduced. In the conductors the alternating current induces eddy currents which shift the current density from the inside towards the outside of conductor. This is the skin effect and is modelled by:

$$J(x) = J(r) \cdot \frac{I_0(\sqrt{j} m \cdot x)}{I_0(\sqrt{j} m \cdot r)} \quad (18)$$

Herein is  $m = \sqrt{\frac{\omega \mu}{\rho_e}}$  and  $x$  the position on the radius.  $\omega$  is defined as  $2\pi f_{elec}$ ,  $\mu$  is the magnetic permeability and  $\rho_e$  is the specific resistivity. The parameter  $r$  is the outer radius of the conductor and  $J(r)$  is the current density on the outer surface. Fig. 7 shows the influence of the radius of the conductor and frequency. In this example copper is used ( $\rho_e = 1.724 \cdot 10^{-8} \Omega m$  and  $\mu = 4\pi \cdot 10^{-7} H/m$ ). Due to the skin effect, the AC resistance  $R_{AC}$  increases with frequency. Using following equation [7]:

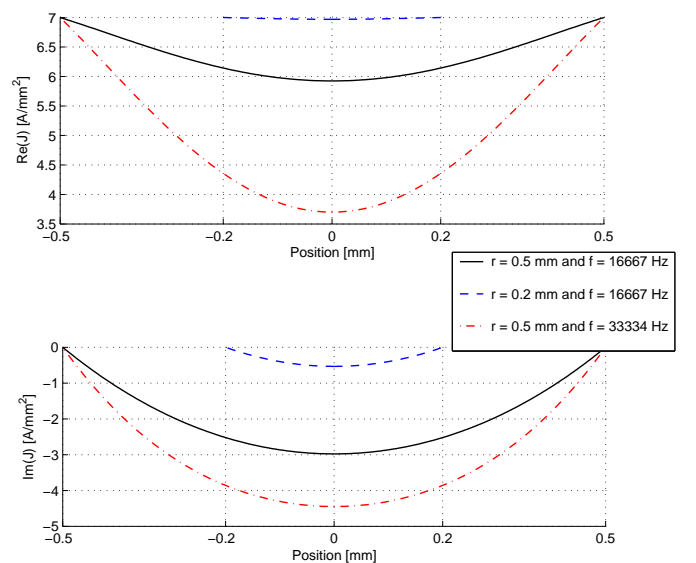


Fig. 7. Current density for the radii  $r = 0.5$  mm and  $0.2$  mm

$$\frac{R_{AC}}{R_{DC}} = \xi \frac{\sinh(2\xi) + \sin(2\xi)}{\cosh(2\xi) - \cos(2\xi)} \quad (19)$$

Herein is  $R_{DC}$  the resistance if DC current was used.  $\xi$  is the normalized conductor height and is equal to  $\frac{h}{\delta}$ , with  $h$  the conductor height and  $\delta$  the skin depth.  $\delta$  is defined as  $\sqrt{\frac{2}{\omega\mu\sigma}}$  with  $\sigma = \frac{1}{\rho_c}$ .

Fig. 8 shows that working with a frequency of  $f = 16,667$  Hz almost doubles the DC resistance value, for  $f = 33,334$  Hz it triples.

The number of poles should therefore be minimized for

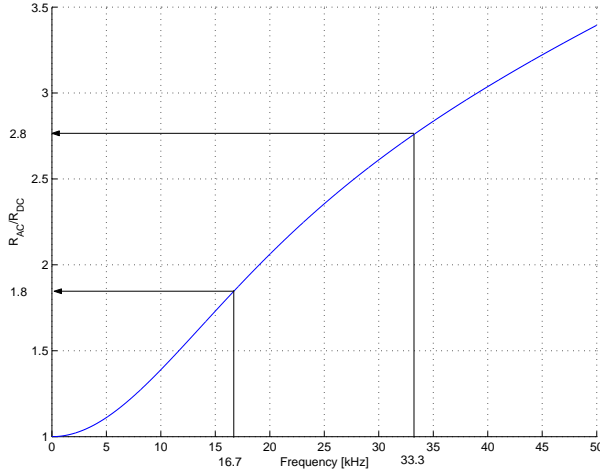


Fig. 8. Increase of resistance as function of frequency

high speed machines, which is obvious. The minimum pole pairs that can be used in this machine is 2. The resulting operating frequency is 16,667 Hz and the corresponding AC-resistance is 1.8 times higher than the DC value.

## V. OPTIMIZATION

In this section a non-linear static optimization is performed. Due to numerical problems the non-linear transient optimization could not be finished in time. Therefore the resulting geometry of the static optimization is used in the transient model to calculate the output power as generator.

Three ratios are used to optimize the electrical micromachine:

$$\frac{P_{mech}}{P_{cop}} \quad (20)$$

$$\frac{P_{mech}}{Vol} = \mathcal{P}_{mech} \quad (21)$$

$$\frac{\mathcal{P}_{mech}}{\mathcal{P}_{cop}} \quad (22)$$

Herein is  $\mathcal{P}_{cop}$ :

$$\mathcal{P}_{cop} = \frac{P_{cop}}{Vol} \quad (23)$$

$\frac{P_{mech}}{P_{cop}}$ , the total power ratio, is the ratio of the total mechanical output power per the total copper loss. If this ratio is maximized, the maximum mechanical output power to copper loss is obtained for a certain volume.

The second ratio  $\mathcal{P}_{mech}$ , the mechanical power density, gives the maximum mechanical output power per unit volume (expressed in  $\text{cm}^3$ ).

The last ratio  $\frac{\mathcal{P}_{mech}}{\mathcal{P}_{cop}}$ , the specific power density ratio, optimizes the use of the material. To determine the power densities, the volumes of the windings and the machine must be calculated. The volume of the machine can be written as (see Fig. 6):

$$Vol = \pi(R_{out}^2 - R_{in}^2)[L_{sb} + L_{ar} + \dots + L_{pm} + L_{ag} + L_{rt}] \quad (24)$$

and the mechanical output power  $P_{mech}$ :

$$P_{mech} = 2N_{slot}B_{air}l_cJN_pA_c\left[\frac{R_{out} + R_{pm}}{2}\right]\omega \quad (25)$$

herein is the air gap flux density  $B_{air}$

$$B_{air} = B_{magn} \frac{\mathfrak{R}_3}{\mathfrak{R}_{tot}} \quad (26)$$

with  $B_{magn}$  the remanent flux density of the permanent magnet and

$$\mathfrak{R}_{tot} = \sum \mathfrak{R}_i \quad (27)$$

The volume of the active conductors is:

$$Vol_{con} = 2N_pN_{slot}R_{con}^2\pi\left[2(R_{out} - R_{pm} - 2R_{con}) + \dots + (R_{pm} + R_{pm})\frac{\theta(N_{slot} + 1)}{N_{slot}}\right] \quad (28)$$

The basic parameters of the linear static DCM analysis are given in Table I. In further analysis, the influence of

Parameter	Value	Dimension
$R_{pm}$	3	[mm]
$L_{pm}$	1	[mm]
$N_{slot}$	1	[-]
$\theta$	$\frac{\pi}{6}$	[rad]
$L_{sb}$	2	[mm]
$L_{ar}$	1	[mm]
$L_{rt}$	2	[mm]
$R_{con}$	0.1	[mm]
$L_{ag}$	0.1	[mm]
$B_{magn}$	1.1	[T]
$N_p$	3	[-]
$\mu_{pm}$	1.1	[-]

TABLE I

BASIC PARAMETERS OF GEOMETRY

some important parameters is studied starting from these basic values. The parameters that are not focused on during the study are equal to the values printed in Table I. The materials that will be used for the construction of the machine must undergo some further testing, mechanical as well as magnetic. It is not necessary to use these special materials to prove the method, therefore a standard steel is implemented.

One of the most significant parameters are  $R_{pm}$  and  $L_{pm}$  which determine the geometry of the permanent magnet. The influence of  $R_{pm}$  and  $L_{pm}$  on the mechanical power density,  $\mathcal{P}_{mech}$ , and the specific power density ratio,  $\frac{\mathcal{P}_{mech}}{\mathcal{P}_{cop}}$ , are shown in Fig. 9 and 10. Both figures show that there is an optimum

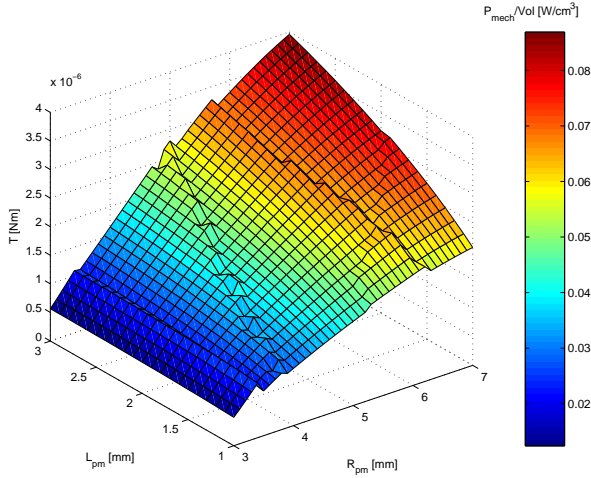


Fig. 9. The torque and the mechanical power density for varying geometry of the PM

permanent magnet size. The explanation for this is that for large sizes of  $R_{pm}$ , the reluctance of the teeth increases. To maintain the high torque and thus the high  $B_{air}$  the length of the permanent magnet  $L_{pm}$  has to increase. The gain in torque compensates the increase in volume so that the overall effect is a gain in the specific power density ratio  $\frac{\mathcal{P}_{mech}}{\mathcal{P}_{cop}}$ . The total power ratio  $\frac{\mathcal{P}_{mech}}{\mathcal{P}_{cop}}$  follows the same trend. For small sizes of  $L_{pm}$  the air gap flux density is not sufficient enough to provide good torque, therefore the specific power density ratio  $\frac{\mathcal{P}_{mech}}{\mathcal{P}_{cop}}$  is decreasing with decreasing  $L_{pm}$ . If  $R_{pm}$  is decreased  $B_{air}$  decreases as well, resulting in a decreasing torque and output power. Another result is shown in Fig. 11. It can be seen that the flux density in the stator and the rotor can be controlled by  $R_{pm}$  for small values of  $R_{pm}$ . For large values of  $R_{pm}$ ,  $L_{pm}$  is the control parameter. The influence of  $L_{rt}$  is obvious, decreasing  $L_{rt}$  increases the flux density in the rotor and decreases the time constant, see section IV because the rotor is pushed deep into saturation. On the other hand the teeth should remain in the linear region. Therefore  $L_{sb}$  must be larger to minimize the losses in the stator back but not too large since it has a negative influence on the specific power density ratio and the mechanical power density. The parameter  $L_{ar}$  is useful if the area available for conductors is too small.

The dimensions resulting of an optimization analysis, are printed in Tables II and III. The high values of the  $B_{rot}$  are clearly a consequence of the small dimensions of  $L_{rt}$ . The geometry of the optimization for the specific power density ratio was subjected to a non-linear FE analysis to validate the DCM-model. The results are shown in Fig. 12. In this figure only the half of the rotor is shown. The results, as can be seen, are in good correspondence.

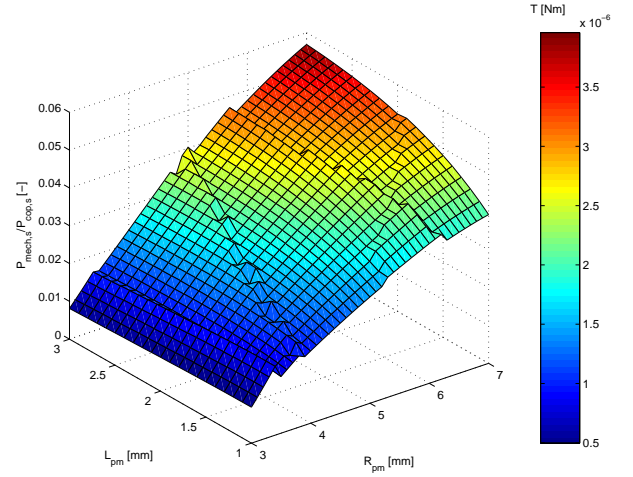


Fig. 10. Specific power density ratio and torque for varying geometry of PM

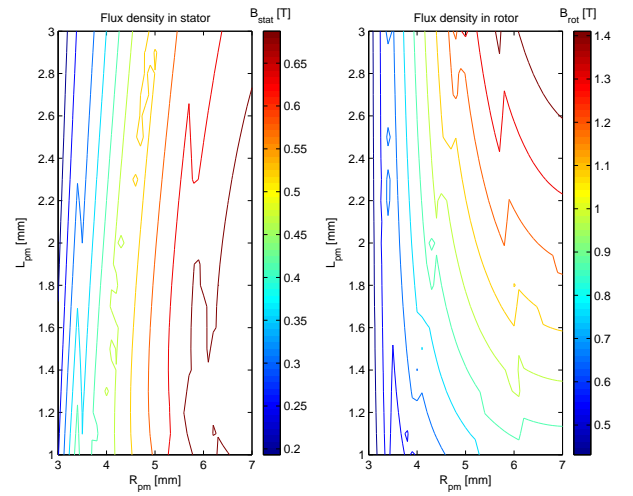


Fig. 11. Flux densities in stator and rotor for varying geometry of PM

Parameter	Value	Dimension
$R_{pm}$	5.5	[mm]
$L_{pm}$	5.0	[mm]
$N_{slot}$	1	[-]
$N_p$	5	[-]
$\theta$	$\frac{\pi}{2}$	[rad]
$L_{sb}$	1	[mm]
$L_{ar}$	7.0	[mm]
$L_{rt}$	2	[mm]
$R_{con}$	1.2	[mm]
$L_{ag}$	0.1	[mm]
$T$	0.002	[Nm]
$\mathcal{P}_{mech}$	23.1	[W/cm <sup>3</sup> ]
$\frac{\mathcal{P}_{mech}}{\mathcal{P}_{cop}}$	28.1	[-]
$\frac{\mathcal{P}_{mech}}{\mathcal{P}_{cop}}$	15.1	[-]
$B_{air}$	0.4	[T]
$B_{stat}$	0.5	[T]
$B_{rot}$	1.6	[T]
$B_{teeth}$	0.5	[T]

TABLE II  
OPTIMIZATION FOR SPECIFIC POWER DENSITY RATIO AND MECHANICAL POWER DENSITY WITH STANDARD STEEL

Parameter	Value	Dimension
$R_{pm}$	6.7	[mm]
$L_{pm}$	8	[mm]
$N_{slot}$	1	[-]
$N_p$	11	[-]
$\theta$	$\frac{\pi}{2}$	[rad]
$L_{sb}$	1	[mm]
$L_{ar}$	7.0	[mm]
$L_{rt}$	1.5	[mm]
$R_{con}$	0.6	[mm]
$L_{ag}$	0.1	[mm]
$T$	0.002	[Nm]
$\mathcal{P}_{mech}$	19.9	[W/cm <sup>3</sup> ]
$\frac{\mathcal{P}_{mech}}{\mathcal{P}_{cop}}$	47.9	[-]
$\frac{\mathcal{P}_{mech}}{\mathcal{P}_{cop}}$	13.0	[-]
$B_{air}$	0.6	[T]
$B_{stat}$	0.4	[T]
$B_{rot}$	2.4	[T]
$B_{teeth}$	0.9	[T]

TABLE III

OPTIMIZATION FOR TOTAL POWER RATIO WITH STANDARD STEEL

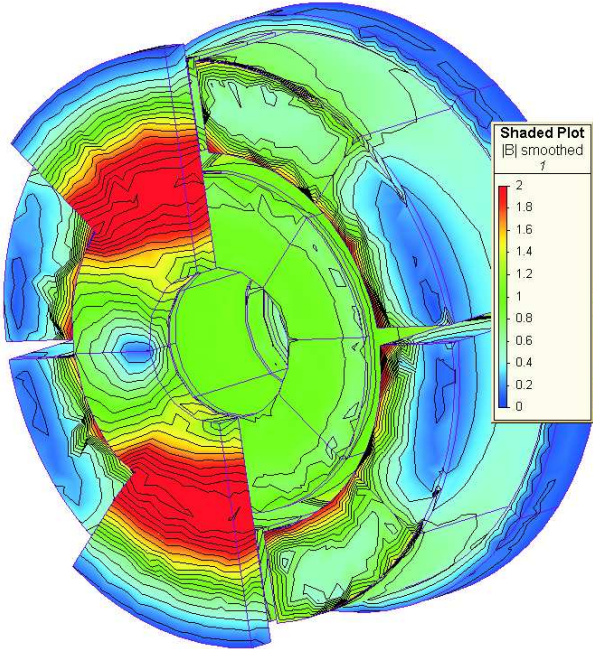


Fig. 12. A non-linear static FE analysis of the optimize geometry for the specific power ratio

## VI. TRANSIENT ANALYSIS

The result of the transient computation is shown in Fig. 13. The micromachine is used as a generator with the dimensions of the optimization for maximum specific power density and mechanical power density. The machine is driven by a torque of 0.002 N from standstill. Only the time interval from 0 to 0.1 s is shown for phase 1. This figure depends on the load that is connected to the machine which is 1000  $\Omega$ , pure resistive. Therefore the electrical power generated by phase 1 is pure active as can be seen in Fig. 14. These figures correspond to an acceleration from 0 to 814 rad.

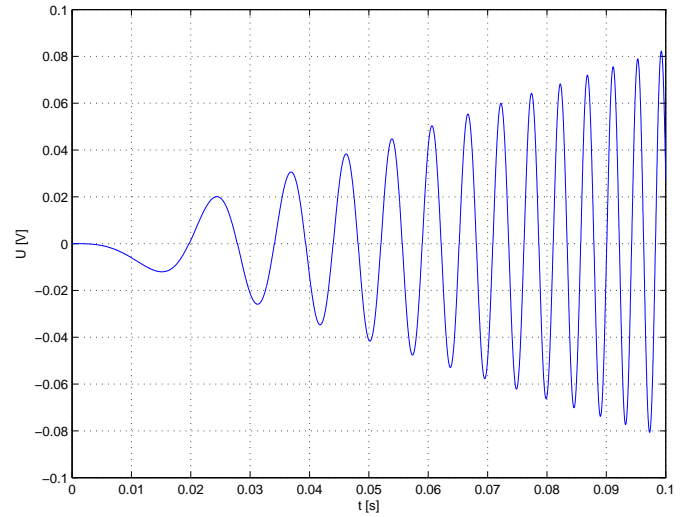


Fig. 13. Voltage of phase 1 during startup to 814 rad

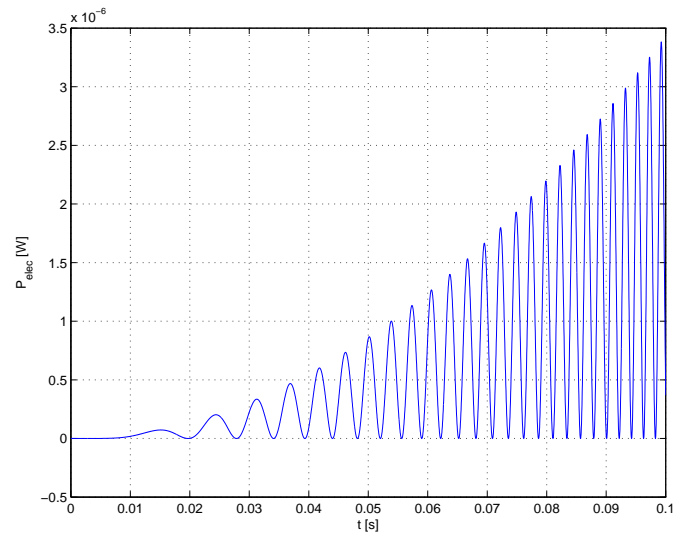


Fig. 14. The electrical power of phase 1 during startup to 814 rad

## VII. CONCLUSIONS

In this paper a non-linear static optimization method of a new hybrid micromachine is presented. This micromachine has a mechanical energy density of 23.1 W/cm<sup>3</sup>, a total power ratio of 28.1 and a torque of 0.002 N if the non-linear model of the micromachine is optimized for specific power density ratio or mechanical power density. If it is optimized for the total power ratio, than the mechanical energy density is 19.9 W/cm<sup>3</sup>, a total power ratio of 47.9 and the torque is 0.002 N. The non-linear FE calculation shows that the non-linear DCM optimization process gives adequate results for the flux densities. In the future, the magnetic properties of the special materials that can withstand the high mechanical stress will be incorporated in the model as well as a thermal analysis.

## VIII. ACKNOWLEDGEMENT

The authors gratefully acknowledge Dr. Ir. G. Deliège bounded to the dep. of Computer Science, div. TWR at the

K.U.Leuven for his contributions to this paper.

#### REFERENCES

- [1] J. Peirs, D. Reynaerts, and F. Verplaetsen, "A microturbine for electric power generation," *Sensors and Actuators A*, no. 113, pp. 86–93, 2004.
- [2] J. Peirs, D. Reynaerts, and F. Verplaetsen, "A micro gas turbine unit for electric power generation: Design and testing of turbine and compressor," in *Technical Digest PowerMEMS 2003*, Third International Workshop on Micro and Nanotechnology for Power Generation and Energy Conversion Applications, (Makuhari, Japan), pp. 19–22, December 2003.
- [3] S. Stevens, J. Driesen, and R. Belmans, "The design of a hybrid high-speed electrical micromachine," in *The Fourth International Workshop on Micro and Nanotechnology for Power Generation and Energy Conversion Applications*, (Japan), November 2004.
- [4] K.U.Leuven, "powermems project." <http://www.powermems.be>.
- [5] E. Hairer and G. Wanner, *Solving ordinary differential equations. 2: Stiff and differential-algebraic problems*. Springer, 1996.
- [6] G. Strang, *Linear algebra and its applications*. Harcourt Brace Jovanovich college publ., 1988.
- [7] V. Ostović, *Computer-aided Analysis of Electric Machines: A Mathematical approach*. Prentice Hall, 1994.



**Ronnie Belmans** (S'77-M'84-SM'89) received the M.S. degree in electrical engineering in 1979, the Ph.D. in 1984, and the Special Doctorate in 1989 from the K.U.Leuven, Belgium and the Habilitation from the RWTH, Aachen, Germany, in 1993. Currently, he is full professor with K.U.Leuven, teaching electrical machines and variable speed drives. He is appointed visiting professor at Imperial College in London. He is also President of UIE. He was with the Laboratory for Electrical Machines of the RWTH, Aachen, Germany (Von Humboldt Fellow, Oct.'88-Sept.'89). Oct.'89-Sept.'90, he was visiting associate professor at Mc Master University, Hamilton, Ont., Canada. During the academic year 1995-1996 he occupied the Chair at the London University, offered by the Anglo-Belgian Society. Dr.Belmans is a fellow of the IEE (United Kingdom). He is the chairman of the board of Elia, the Belgian transmission grid operator.



**Stijn Stevens** (S'98-M'03) received the M.S. degree in electro-mechanical engineering in 2003 with specialization Aerospace engineering. Currently he is working toward his Ph.D in electrotechnical engineering at the K.U.Leuven division ELECTA.



**Johan Driesen** (S'93-M'97) graduated as an Electrotechnical Engineer and received the Ph.D. degree in electrical engineering from the Katholieke Universiteit Leuven (KULeuven), Leuven, Belgium, in 1996 and 2000, respectively. In 1996, he became a Research Assistant of the Fonds voor Wetenschappelijk Onderzoek-Vlaanderen (Fund for Scientific Research of Flanders - F.W.O.-VI.). From 2000 to 2001, he was a Visiting Lecturer with Imperial College, London, U.K. In 2002, he was a Visiting Scholar with the Electrical Engineering Department, University of California at Berkeley. He is currently a Postdoctoral Research Fellow of the F.W.O.-VI. at KULeuven. Dr. Driesen received the 1996 R&D Award of the Belgian Royal Society of Electrotechnical Engineers (KBVE) for his Master's thesis on power quality problems. In 2002, he received the KBVE R. Sinave Award for his Ph.D. dissertation on coupled problems in electrical energy transducers.